ISSN (Print) 1226-1750
ISSN (Online) 2233-6656
Journal of Magnetics 24(3), 518-529 (2019) https://doi.org/10.4283/JMAG.2019.24.3.518

Sensing Magnetic Fields With Surface Acoustic Wave (SAW) Sensors

Fayyaz Muhammad[1,2] and Hu Hong[1]*

[1]*School of Mechanical Engineering and Automation, Harbin Institute of Technology, Shenzhen, Shenzhen, Guangdong 518055, China*
[2]*Electronics Division, Pakistan Institute of Nuclear Science and Technology (PINSTECH), Islamabad, Pakistan*

(Received 17 October 2018, Received in final form 16 July 2019, Accepted 23 July 2019)

Magnetic sensors are essential sensing elements in various industrial applications, but the design and technology used in the development of these sensors vary from application to application. Recently Surface Acoustic Wave (SAW) sensors have gained considerable attention due to their advantages over conventional sensors. SAW sensors are a class of Microelectromechanical (MEMS) system that use SAW technology and can be easily configured to sense physical parameters including magnetic fields. This paper presents an overview of recent research in the domain of magnetic field sensing based on such SAW devices. The paper describes the most common design approaches in practice and also discusses the key properties of fabrication materials for optimum design and performance. A short review of the processes involved in the development of SAW magnetic sensors is also covered in this paper.

Keywords: magnetic field sensor, SAW sensor, piezoelectric, magnetostriction, MEMS

1. Introduction

Magnetic sensors are vital measurement components in various industrial, engineering and scientific applications. These sensors are installed or incorporated within devices and systems to sense magnetic fields and their vector components [1]. Magnetic sensors have wide range of application areas including automotive [2], security [3], navigation [4], automation [5], date storage [6], biomedical [7], machines fault monitoring [8] and non-destructive testing [9]. Magnetic sensors design and functionality rely on different theoretical phenomenon [10]. The most common magnetic sensors found in the literature are: Fluxgate [11], Magnetoinductive [12], Superconducting Quantum Interference Device (SQUID) [13], Search Coil [14], Hall Sensor [15], Magnetoresistors [16], Anisotropic Magnetoresistive (AMR) [17], Spin-Dependent Tunneling (SDT) [18] and Giant Magnetoresistive (GMR) [19]. These sensors use diverse design technologies and demonstrate supremacy over one another in terms of sensitivity, robustness, resolution, construction, and cost. These characteristics restrict their usage to a specific application and are chosen considering the application specific requirements.

Recent advances in technology have revolutionized measurement science and technology. The growing trend of developing compact, power efficient and low-cost devices with improved performance has led to the fusion of multidiscipline technologies and has broadened the research scope. Against this background, magnetic sensors being developed today also exploit state-of-the-art technologies to provide optimum sensing solutions. Microelectromechanical Systems (MEMS) is one such promising technology that has made a prominent contribution to the development of smaller and low-cost devices for various industrial applications [20]. In Particular, MEMS technology has played a significant role in the production of a new generation of magnetic sensors [21, 22].

In recent years, a class of MEMS known as Surface Acoustic Wave (SAW) devices has gained a good reputation in sensor technology. Usage of SAW devices is growing and they have become part of many electronic devices and systems used for sensing physical parameters [23-28]. SAW sensors are preferred over conventional sensors due to their miniature size, higher sensitivity, simple design and versatility [29]. The basic structure of a SAW sensor is shown in Figure1. The Interdigital Transducer (IDT) electrodes produce strain and compression on the piezoelectric substrate surface when an alternating current (AC) voltage or signal is applied between them. As a result of alternate electrical potential at the electrodes,

*Corresponding author: Tel: +86-755-26033811
Fax: +86-755-26032774, e-mail: honghu@hit.edu.cn

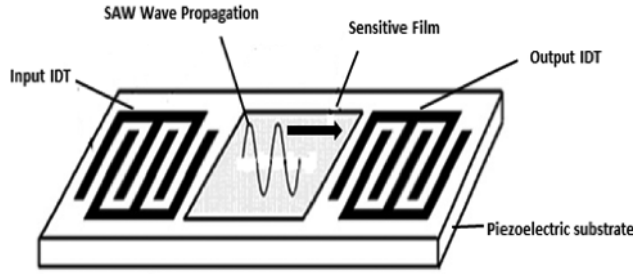

Fig. 1. Basic two-port SAW sensor with delay line structure.

mechanical waves i.e. SAWs are generated which travel along the surface of the piezoelectric substrate. When SAWs interact with IDTs, a reverse phenomenon is observed and mechanical energy is converted back to an electrical signal or alternating voltage. The physical quantity being measured is sensed by observing the variations in the signal at the output IDT port. These variations are the result of changes occurred in the form of shifts in velocity, phase and frequency of propagating SAWs because of the influence of measuring physical quantity on sensitive film within the SAW device. SAW sensors have been in use for several decades and are able to operate in both active and passive modes. Passive SAW devices benefit from wireless technology by getting power and exchanging signals, which make them suitable for remote sensing applications [30-32].

Due to their proven worth in various applications, SAW sensors have been adopted for sensing magnetic fields and have become an emerging area of research. Although SAW magnetic sensors have not been commercialized and most of the work in this domain is still in the laboratory, a review of relevant literature reveals that SAW magnetic sensors are gaining popularity and have the potential to outclass conventional magnetic devices. The main research on SAW magnetic sensors revolves around sensor materials, structure design, and sensing methods. The following sections of this paper discuss the SAW magnetic sensors in detail. Section 2 covers the common SAW magnetic sensor design approaches in practice, which includes a discussion of the performance and results achieved, while section 3 provides an overview of fabrication techniques associated with SAW magnetic sensor development.

2. SAW Magnetic Sensors

SAW magnetic sensors have a similar basic structure like general SAW sensor as shown in Figure 1. SAW magnetic sensors are composed of the piezoelectric substrate, Interdigital Transducers (IDT) and an embedded sensing element within the SAW device which is a material sensitive to magnetic fields. SAW magnetic sensors may also include reflectors [33] and absorbers [34] for SAW reflections and unwanted waves absorptions respectively depending on the device configuration used. The sensing element is a key component of measurement which introduces variations in the characteristics of propagating SAWs upon the application of an external magnetic field and then these variations are translated as the magnitude of the magnetic field. During the sensor operation, the SAW travels along the surface of the piezoelectric substrate. The equation of motion governing this mechanical wave in the absence of external forces for a perfectly elastic, homogenous and anisotropic medium, is expressed as (Eq. 1) where ρ is the density of the medium, u_i is the displacement along the axes and T_{ij} is the stress tensor.

$$\rho\frac{\partial^2 u_i}{\partial t^2} = \frac{\partial T_{ij}}{\partial x_j} \quad \text{i, j =1,2,3} \tag{1}$$

The propagating wave characteristics depend on the properties of the piezoelectric substrate material. Therefore the crucial parameters associated with piezoelectric substrates, such as electro-mechanical coupling coefficient, wave velocity, temperature coefficient of delay and functional frequency, are of great concern when selecting a substrate for sensors design. These parameters depend not only on the inherent properties of substrate materials but also on the orientation or the angular cut of the crystalline structure of substrates, which subsequently defines the axis and angle of the wave propagation [35]. The electromechanical coupling coefficient [36] of the material defines its ability to convert electrical signals into mechanical surface waves. The electromechanical coupling coefficient of piezoelectric substrates can be calculated using the material parameters, such as piezoelectric, elastic, and dielectric constants [37]. Mathematically, the electromechanical coupling coefficient K^2 is defined as:

$$K^2 = 2\frac{V_f - V_m}{V_f} \tag{2}$$

In (Eq. 2) above, V_f and V_m are SAW velocities at the free surface and metallic surfaces respectively. Materials with higher values of electromechanical coupling coefficients are preferred for more efficient sensor design. The SAW velocity [38] parameter corresponds to the speed of the SAW through the material. In addition, the SAW velocity is also useful in determining the sensor's optimum operating frequency at which the sensor has a maximum response. The temperature coefficient of delay (TCD) [39] represents the effect on wave propagation through

the material due to varying temperatures. The lower the value the more stable or fewer disturbances in the wave propagation. There are various materials reported in the literature that have been used as the substrate in SAW sensors. Lithium Niobate and Quartz are the most common substrates. Some other substrate materials that can be employed for SAW magnetic sensors, along with their properties are listed in Table 1 [40].

Interdigital Transducers (IDT) are other essential components of SAW magnetic sensors. IDTs are composed of comb-shaped uniformly spaced arrays of metallic electrodes or fingers placed normally to the SAW propagation axis (see Figure 1). The periodic spacing between electrodes at the same potential is known as pitch and is equal to the wavelength corresponding to the central operating frequency of the sensor. The pitch p and the operating frequency have the following relation:

$$f = v/p \tag{3}$$

where v is SAW velocity within the substrate. The IDT electrodes produce strain and compression on the piezoelectric substrate surface when an alternating current (AC) voltage or signal is applied between them. As a result of alternate electrical potential at the electrodes mechanical waves i.e. SAWs are generated which travel along the surface of the piezoelectric substrate. When SAWs interact with IDTs, the reverse phenomenon is observed and mechanical energy is converted back to an electrical signal or alternating voltage. As mentioned earlier, this transformation of energy is greatly influenced by the material's characteristics. Metals with higher conductivity, low cost and ability to be deposited well on piezoelectric substrates are recommended for the IDTs. Table 3 [41] shows a list of materials that are commonly used in the development of IDTs due to their appealing properties.

SAW resonators [42] and two-port SAW delay line devices [43] are well-known variants of SAW devices. Most SAW magnetic sensors have been designed using diverse design methodologies and utilize the functionality and features of these devices. The literature reveals that SAW magnetic sensors are the devices that measure the magnetic field component and not the total magnitude of the magnetic field. In addition, the sensitivity of SAW magnetic sensors is not only dependent on the material of the sensitive element but also their position and orientation with respect to the direction of the external magnetic field component. In comparison with conventional magnetic sensors SAW magnetic sensors are suitable for detecting magnetic fields ranging between μT and mT while operating at frequencies in MHz and few GHz ranges as reported in recent research papers.

SAW magnetic sensors have a simple structure and can be easily configured for application-specific requirements. From the functioning perspective, SAW magnetic sensors can either be used as an active device or passive device. However, from the design point of view SAW magnetic sensors can be categorized into three main types based on their sensing mechanism.

2.1. Thin Film Based Design

Thin film based SAW magnetic sensor designs are implemented using thin films of magnetostrictive materials, which hold an inherent characteristic that causes them to change their shape or dimension under the influence of an external magnetic field. This change is due to the internal strains generated within the materials due to the rotation

Table 2. (Color online) SAW magnetic sensor comparison with common magnetic sensors.

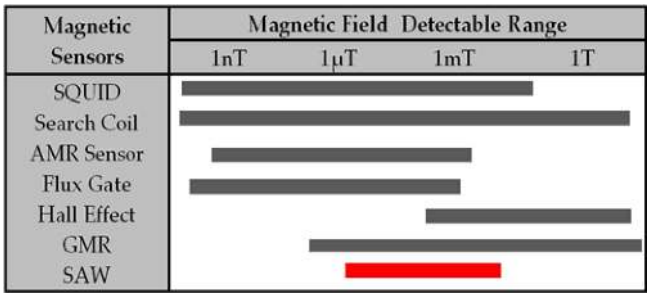

Table 1. Common piezoelectric substrates and their parameters.

Piezoelectric substrate material	Crystal cut	SAW axis	Velocity (m/s)	K^2 (%)	Temp. Coeff. (ppm/°C)	Capacitance/Finger Pair/Unit length C_o (pF/am)
Quartz	ST	X	3158	0.11	~0 near 245°C	0.55
Lithium Niobate $LiNbO_3$	Y	Z	3488	4.5	94	4.6
	128°	X	3992	5.3	75	5.0
Bismuth Germanium Oxide $Bi_{12}GeO_{20}$	110	001	1681	1.4	120	-
Lithium Tantalate $LiTaO_3$	77.1° Rotated Y	Z	3254	0.72	35	4.4
Gallium Arsenide GaAs	(100)	<110>	< 2841	< 0.06	35	-

Table 3. Materials for IDT fabrication.

Metal name	Substrate adherence (Qualitative)	Electrical resistivity (μΩ-cm)	Boiling point (K)	Cost (Qualitative)
Copper	Good	1.7	3200	Low
Aluminum	Good	2.65	2792	Low
Gold	Poor	2.2	3129	High
Tungsten	Average	5.0	5828	Mid
Titanium	Good	50	3560	Mid

and reorientation of magnetic domains [44-46]. In the linear region of sensing the constitutive equations of magnetostriction are given by:

$$S = s^H s + d H \quad (4)$$

$$B = d s + \mu^s H \quad (5)$$

where S is the strain, s the mechanical stress, H the magnetic field intensity and B the flux density. The compliance value at a constant magnetic intensity is denoted by s^H, d is the magneto-mechanical constant, and μ^s is the permeability of the medium under constant stress condition. There is a wide range of magnetostrictive materials and their alloys that are used in sensors and actuators, some of which along with their magneto-elastic properties are presented in Table 4 [47].

Magnetic sensors designed using the thin film scheme exploit two-port-delay line structures, with thin film deposited in the delay line between the input and output IDTs of the sensor. When the SAW magnetic sensor is exposed to external magnetic field H, the magnetostrictive film in the SAW propagation path changes its dimension along the direction of the external magnetic field. Stresses are consequently generated on the underlying substrate, which results in increased strains affecting SAW characteristics i.e. phase shift, velocity and amplitude. These changes are observed in the output signal, which indicates the magnetic field strength. In the thin film based SAW magnetic sensors, SAW relative velocity change (Δv/v) is the most studied feature to measure the magnetic field strength and analyze the sensitivity of the sensors.

Researchers [48] have demonstrated SAW phase shift using Nickel(Ni) as the magnetostrictive thin film in the delay line of a SAW device developed on Lithium Niobate ($LiNbO_3$) substrate. They showed that the SAW velocity can be varied by controlling the external magnetic field. The effects on velocity change have also been studied [49] in which the alloys of (Tb, Dy)Fe_2 were used as magnetostrictive thin films and were deposited on a $LiNbO_3$ substrate; the magnetostriction of these films and relative velocity change with respect to the external magnetic field was examined. The results showed the

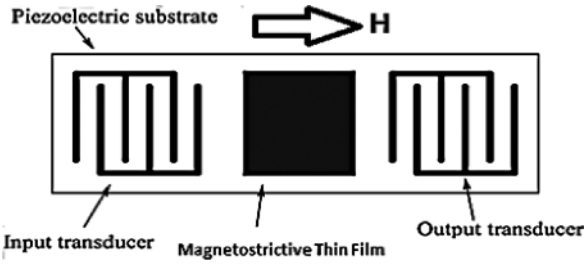

Fig. 2. Basic SAW magnetic sensor design using thin film.

Table 4. Important magnetostrictive materials and their properties.

Material	$3/2\,\lambda_s$ ($\times 10^{-6}$)	ρ (g/cm^3)	B_s (T)	T_c (°C)	E (GPa)	k
Fe	–14	7.88	2.15	770	285	
Ni	–50	8.9	0.61	358	210	0.31
Co	–93	8.9	1.79	1120	210	
50%Co-50%Fe	87	8.25	2.45	500		0.35
50%Ni-50%Fe	19		1.60	500		
$TbFe_2$	2630	9.1	1.1	423		0.35
Tb	3000(–196°C)	8.33		-48	55.7	
Dy	6000(–196°C)	8.56		-184	61.4	
Terfenol- D	1620	9.25	1.0	380	110	0.77
$Tb_{0.6}Dy_{0.4}$	6000					
Metglass 2605SC	60	7.32	1.65	370	25-200	0.92

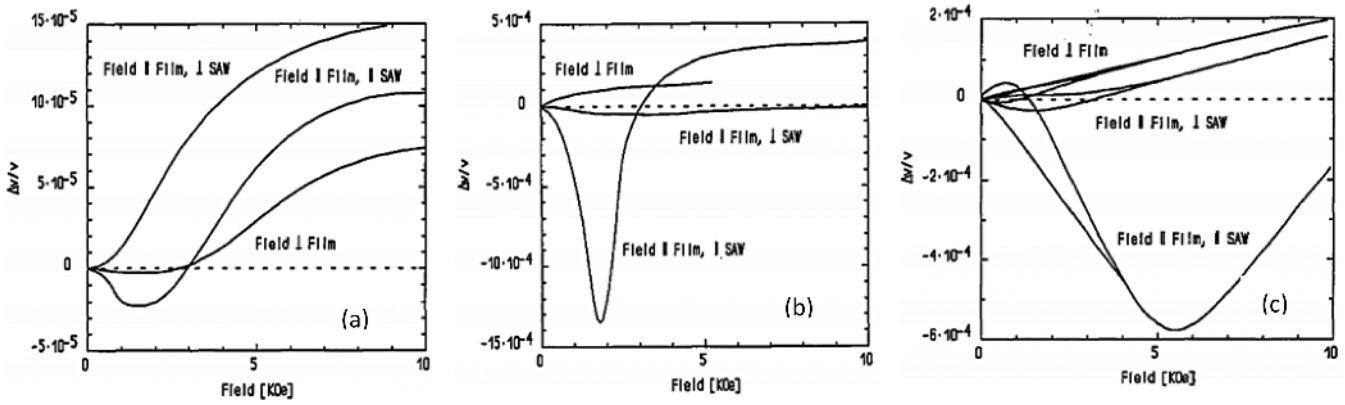

Fig. 3. Relative velocity changes due to different alloys of (Tb,Dy)Fe_2 (a) $Tb_{0.7}Dy_{0.3}Fe_2$0.48 μm thick (b) $Tb_{0.3}Dy_{0.7}Fe_2$ 4.9 μm thick (c) $TbFe_2$ 1.9 μm thick

dependency of a relative velocity change on the orientation of the thin films with respect to the direction of the sensing magnetic field which is demonstrated in Figure 3.

Galfenol is another well-known magnetostri-ctive material with unique properties making it promising for sensing applications [50, 51]. Galfenol is the general name for an alloy of Gallium and Iron. The magnetostriction values of Galfenol varies over a wide composition range $Fe_{1-x}Ga_x$ ($0.04 \leq x \leq 0.35$) [52]. Li *et al.* [53] demonstrated the use of Galfenol as a thin film in SAW magnetic sensors. The fabricated SAW devices designed to operate at 158 MHz frequency on a quartz substrate with Galfenol thin films of variable length and thickness. They achieved up to 0.64 % of SAW velocity change with the film thickness of 500 nm which is claimed to be greater than the previous results reported for similar sensor types. The researchers observed that the maximum velocity occurred at the coercivity field of the Galfenol thin film and experimentally showed that thicker Galfenol films exhibited larger velocity change, which can be seen in Figure 4(b). Mathematically, this relative change in SAW velocity in case of the acoustically thin films is given by the Tiersten formula [54]:

$$\frac{\Delta V}{V} = -\omega h \sum_{i=1}^{3} c_i \left(\rho - \frac{E^{(i)}}{V^2} \right) \tag{6}$$

where ω is the SAW frequency and h the film thickness. The SAW-film coupling parameter c_i, and moduli, $E^{(i)}$, associated with strain modes are constant in the i^{th} (x, y, or z) displacement component for a specific film. The researchers also found that thin and thick films are determined by a criterion which is the ratio of strains caused by cross-film displacement gradient and the strain caused by the in-plane gradient. Mathematically this is expressed as:

$$R = \frac{A f v_0 \rho h}{|G|} \tag{7}$$

where A is a parameter depending on the substrate and is 1.9 for ST-cut quartz. f, v_o, ρ, h, and G are the frequency, wave velocity, film density, film thickness, and film shear modulus respectively. All the Galfenol thin films used in

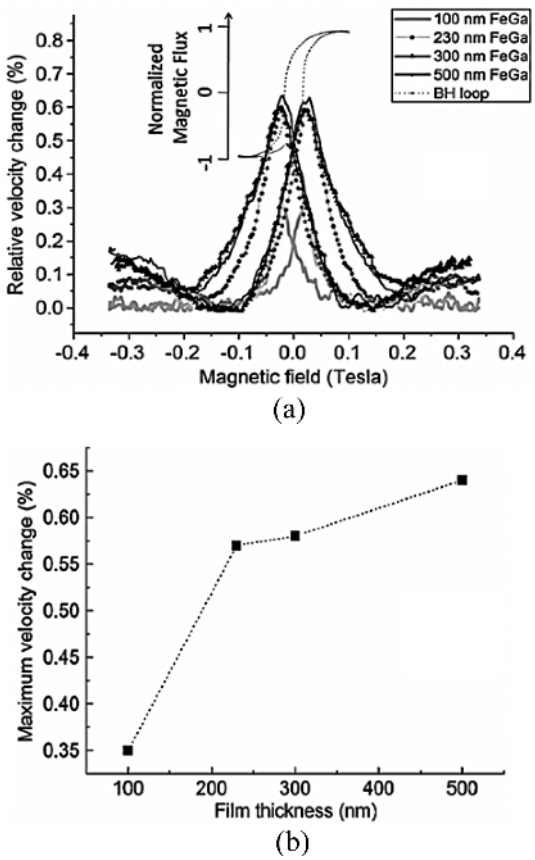

Fig. 4. Relative velocity change observed using Galfenol thin film: (a) comparison plot of velocity change for different film thickness (b) maximum velocity change with respect to the film thickness.

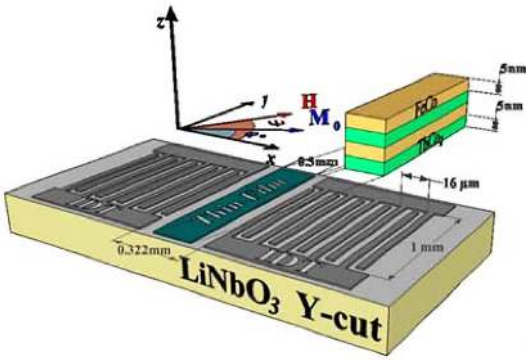

Fig. 5. (Color online) SAW device with a multilayered thin film.

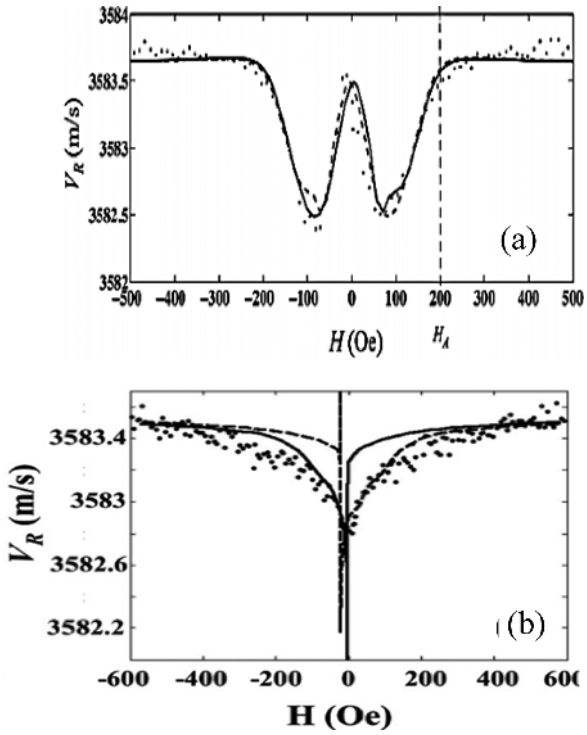

Fig. 6. Velocity shifts due to $TbCo_2$/FeCo nanostructured uni-axial films (a) for magnetic field along the hard axis (b) for magnetic field along the easy axis.

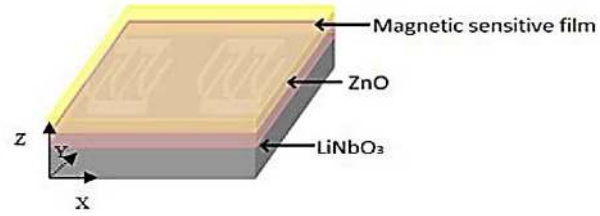

Fig. 7. (Color online) Basic layout of a layered structure.

the experiments satisfied (Eq. 7) and the ratio calculated was less than 1. Hence they were all considered thin films and (Eq. 6) is applicable to them for studying Δv/v.

Recently, the concept of using a thin film of magnetostrictive material has reformed and multilayer thin films are being deposited in SAW magnetic sensors for improved sensitivity. Zhou *et al.* [55] developed SAW devices using multilayer films deposited in SAW delay line on Y-cut $LiNbO_3$ substrate. The multilayer deposited films consisted of 20 x $TbCo_2$/FeCo nanostructured uni-axial films and were used in the configuration as shown in Figure 5. The researchers measured and calculated the phase velocity variations for the external magnetic field of variable strength and direction i.e. hard and easy axes. The authors also studied the magnetization induced in the above structure along both easy and hard axes.

Elhosni *et al.* [56] developed a SAW magnetic sensor using a layered structure of Ni/ZnO/IDT/$LiNbO_3$and CoFeB/ZnO/IDT/ $LiNbO_3$. As can be seen from Figure 7, the bottom layer was of $LiNbO_3$ substrate with IDTs fabricated on it, followed by a 250 nm thick layer of ZnO and then a 200 nm thick layer of Ni or CoFeB.

The magnetization of both sensitive layers was studied and it was observed that the CoFeB has better magnetization but a lower saturation field as compared to Ni. It can be seen from Figure 8 that Ni is isotropic in the X-Y plane whereas CoFeB showed its hard axis along X and easy axis along Y.

The experiments included the study of variations in

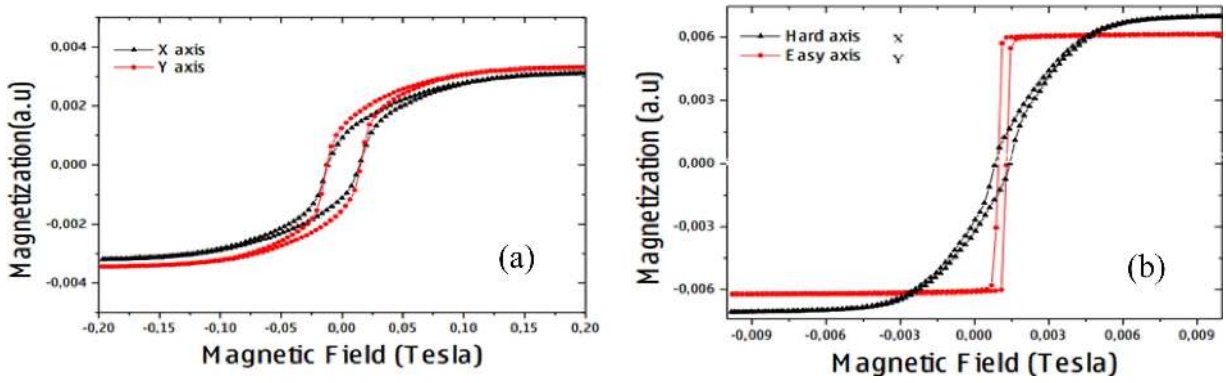

Fig. 8. (Color online) Magnetization curves (a) Ni film (b) CoFeB film.

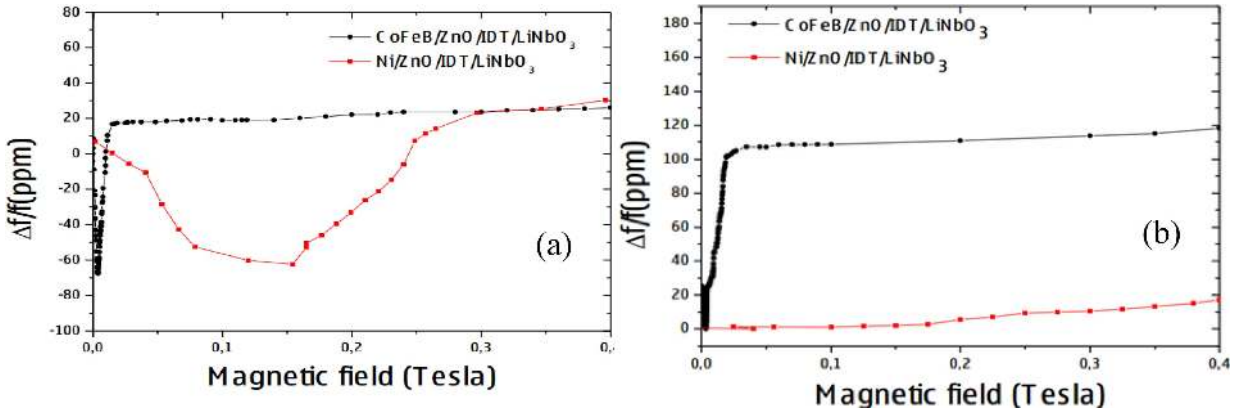

Fig. 9. (Color online) Relative Frequency Change (a) For parallel magnetic field (b) For perpendicular magnetic field.

relative frequency change due to an applied external magnetic field. The data was recorded for both parallel and perpendicular directions of the magnetic field with respect to the sensitive film. The comparative result in Figure 9 shows that CoFeB qualified for higher sensitivity and suitability for lower magnetic fields.

2.2. Interrogation Based Designs

Interrogation based sensors use the basic structure of a SAW sensor but in a different configuration than that of thin film based designs. Sensors following this design approach retrieve the measurand information contained in the SAW reflections. Unlike thin film based sensors these sensors use input IDT as a transceiver that serves as both input and output port. On reception of an interrogation or input signal at the transceiver port, the SAW is generated and travels towards the device ends where it is reflected back by the reflectors towards the transceiver IDT. These reflected SAWs or the response signals received at the transceiver port carry SAW propagation and reflection properties. The measurand influences these properties and hence by analyzing the response signal, information about the physical parameter is deduced. The working principle enables these kinds of SAW sensors to operate in a passive mode using wireless communication systems. In this mode, the interrogation signal is transmitted from a remote wireless source and is received by a SAW sensor through an antenna connected to the transceiver IDT. This signal energizes the sensor and serves as its interrogation signal. Similarly, the response signals generated by the sensor are transmitted back to the remote receiver through the connected antenna with a transceiver IDT, which are then analyzed for information inferences [57-59].

In order to use interrogation-based sensors to sense physical parameters, sensitive elements are integrated with the sensors' reflectors as a load and are electrically

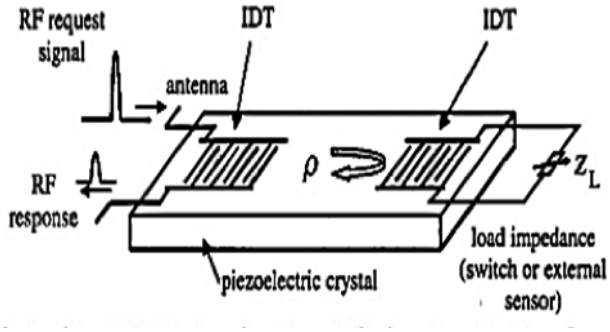

Fig. 10. Basic structure of an interrogation based wireless SAW sensor design in passive mode.

matched with them by tuning the matching circuit. Unmatching in load due to variations in response to changes in the physical phenomenon of interest affects the reflected SAW characteristics. In SAW magnetic sensors the common integrated sensing elements are materials that demonstrate the Giant Magnetoimpedance (GMI) effect. Since GMI materials exhibit large changes in their electrical impedance when exposed to a magnetic field and are also sensitive to applied stresses, it is possible to design and produce GMI-based sensors for various applications [60-62]. The relative impedance change due to the GMI effect in materials is expressed as a GMI ratio that is given as:

$$\text{GMI Ratio (\%)} = 100\ \% \times \frac{Z(H) - Z(H_{\max})}{Z(H_{\max})} \qquad (8)$$

where $\boldsymbol{Z(H)}$ and $\boldsymbol{Z(H_{max})}$ correspond to the impedance at the current intensity of the magnetic field and impedance at the saturation magnetic field respectively. For GMI sensors, amorphous magnetic alloys Co and Fe have been used but NiFe compounds are now preferred due to their high permeability values, zero magnetostriction and ease of fabrication. Some multilayer materials for GMI sensing

Table 5. Data of materials for GMI sensors.

Material	Frequency	GMI Ratio (%)	Sensitivity (%/Oe)
FeNiCrSiB/Cu/FeNiCrSiB	13 Mhz	77	2.8
FeSiBCuNb/Cu/FeSiBCuNb	13 MHz	80	2.8
$Ni_{81}Fe_{19}$/Au/$Ni_{81}Fe_{19}$	300 MHz	150	30
($Ni_{81}Fe_{19}$/Ag)n	1.8 GHz	250	9.3
FeCuNbSiB/SiO_2/Cu/SiO_2/FeCuNbSiB	5.45 MHz	33	1.5
NiFe/Ag/NiFe	1.8 GHz	55	1.2
NiFe/Cu/NiFe	20 MHz	166	8.3

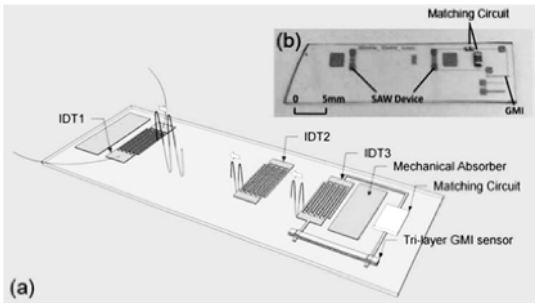

Fig. 11. GMI integrated Wireless SAW magnetic sensor (a) Design layout (b) Integrated sensor.

are listed in Table 5 below [63].

Li *et al.* [64] developed a SAW magnetic sensor by integrating a tri-layered GMI structure($Ni_{80}Fe_{20}$ 100 nm/Cu 200 nm/$Ni_{80}Fe_{20}$ 100 nm) with a wireless SAW device on a common substrate. Their design included a matching circuit to match the impedance of the GMI structure with the IDT port serving as a reflector at the operating frequency of the SAW device. During the sensor operation, an externally applied magnetic field resulted in the deterioration of this matching and affected the amplitude of the reflected SAW. As the SAW characteristics are sensitive to temperature and environmental changes, an additional reference IDT in the SAW delay line was introduced to compensate for temperature effects and to ensure that the observed attenuation in the SAW is due to the effect of magnetic fields only.

The other possible way of designing a GMI-SAW magnetic sensor is to connect a GMI element externally i.e. not fabricated on the SAW device substrate. This design approach was followed by Hauser *et al.* [65] who designed their sensor using amorphous FeCoSiBNd GMI wire connected externally as a load impedance with a two-port SAW device. The sensor also included two unloaded reflectors to circumvent the ambiguity of the phase and temperature effects. The sensor layout is shown in Figure 12 below:

For the maximum transfer of energy, Hauser *et al.* also used matching capacitance in connection with GMI wire and IDT (R2). The operating frequency of the device was 434 MHz and a 13 mm long by 30 μm diameter GMI wire was connected as a sensing element. The researchers studied the relationship between amplitude variations in the SAW reflections and the applied magnetic field and analyzed the performance of their device. They found that variations in the external magnetic field affected the reflected SAW amplitudes due to impedance variations as a result of the GMI effect in the sensing element. These amplitude variations due to the influence of external magnetic field were measured by using:

$$A_{\mathrm{rel}}(\mathrm{dB}) = 20\ \log\left|A_{\mathrm{IDT2}}/A_{\mathrm{ref}}\right| \tag{9}$$

where $\mathbf{A_{IDT2}}$ is the amplitude corresponding to reflections from IDT (R_2) and $\mathbf{A_{ref}}$ is the amplitude corresponding to

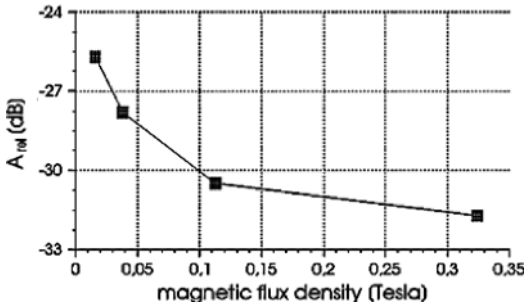

Fig. 13. Amplitude variations of reflected SAW VS External Magnetic field.

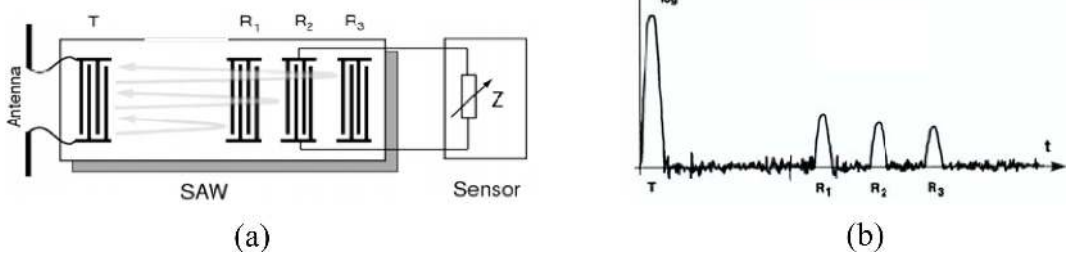

Fig. 12. (a) Schematic layout of GMI-SAW magnetic sensor with GMI wire as load impedance (b) Impulse response of the device

reflections from reference IDT.

2.3. Resonator Based Design

SAW magnetic sensors can also be realized following the SAW resonator design in which the resonance frequency of the resonator is dependent on the SAW velocity through the piezoelectric substrate and the pitch of the IDT as in (Eq. 3). The main feature of this sensor is the IDT design which uses magnetostrictive material instead of conventional metal IDTs. When the sensor is exposed to an external magnetic field, the magnetostrictive IDT electrodes change their dimension along the direction of the magnetic field, which varies the gap between electrode fingers and shifts the resonance frequency. This deviation in resonance frequency quantifies the strength of the magnetic field.

Kadota *et al.* [66] developed a SAW magnetic sensor based on SAW resonators using Ni IDT electrodes and quartz substrate; it was part of a passive and wireless sensing system that was able to read at a range of 3 m. Michio *et al.* [67] also demonstrated a magnetic field measurement method based on a one-port SAW resonator and implemented their design using Ni as the material for a resonator IDT fabricated on ST-90^{0}X quartz.

They studied three kinds of Ni electrode structures on the ST-cut 90^{0}X quartz, namely, (a) grooved Ni electrodes, (b) additional overlaid Ni films on grooved Ni electrodes and (c) Ni electrode, which gave them insight into the most suitable structure for better sensor performance.

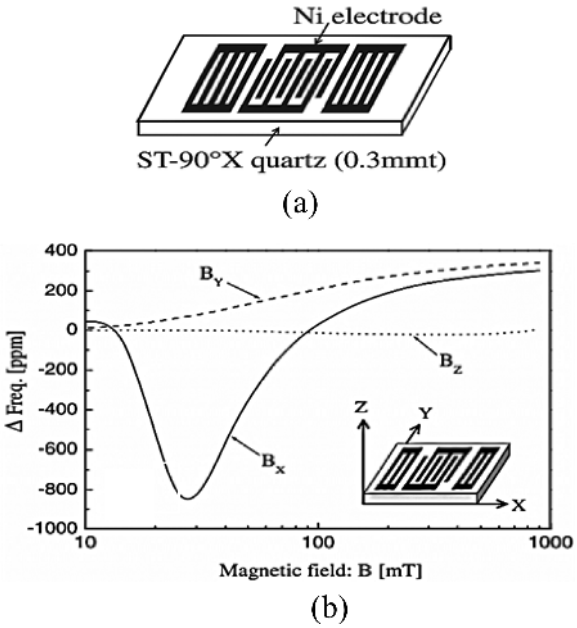

Fig. 14. (a) The layout of Magnetic sensor using one port SAW resonator (b) Sensor response as resonance frequency shift for different values of the magnetic field.

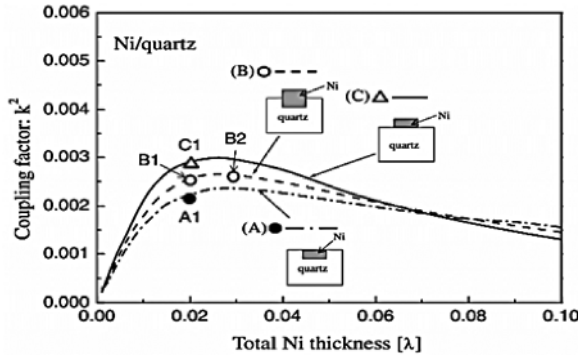

Fig. 15. Coupling factor of various Ni electrode structures (A) grooved Ni electrodes, (B) additional overlaid Ni films on grooved Ni electrodes, and (C) Ni electrode.

3. Fabrication of SAW Magnetic Sensors

SAW magnetic Sensors are fabricated using the standard microelectronic fabrication technologies [68]. The sensor prototype development consists of multiple steps and involves various processes. A summary of the fabrication process steps of a typical thin film based SAW magnetic sensor is provided in below.

Step 1: Wafer Cleansing

The bare wafer of the piezoelectric substrate is the bottom layer or initial stage of sensor fabrication. The wafer surface is cleaned with a cleansing agent (e.g. Acetone Isopropyl deionized water or Acetone Methanol deionized water) to remove containments.

Step 2: Metal Deposition

By Evaporation/Sputtering/chemical vapor deposition (CVD) process a uniform layer of metal, e.g. Aluminum, is deposited on the top of the piezoelectric wafer. This is required for the development of Interdigital transducers (IDTs).

Steps 3: Photoresist spin-on and UV exposure

A layer of photoresist material is applied on top of the metal layer developed in the previous step using Photolithography process. The photoresist layer is exposed to UV light. A photomask (chrome or Mylar) is used to place the desired IDT pattern on the metal layer.

Step 4: Etching metal layer

Using Dry/Wet Etching process portions of the photoresist layer unprotected by the mask are washed away using a developer solution exposing the layer of metal

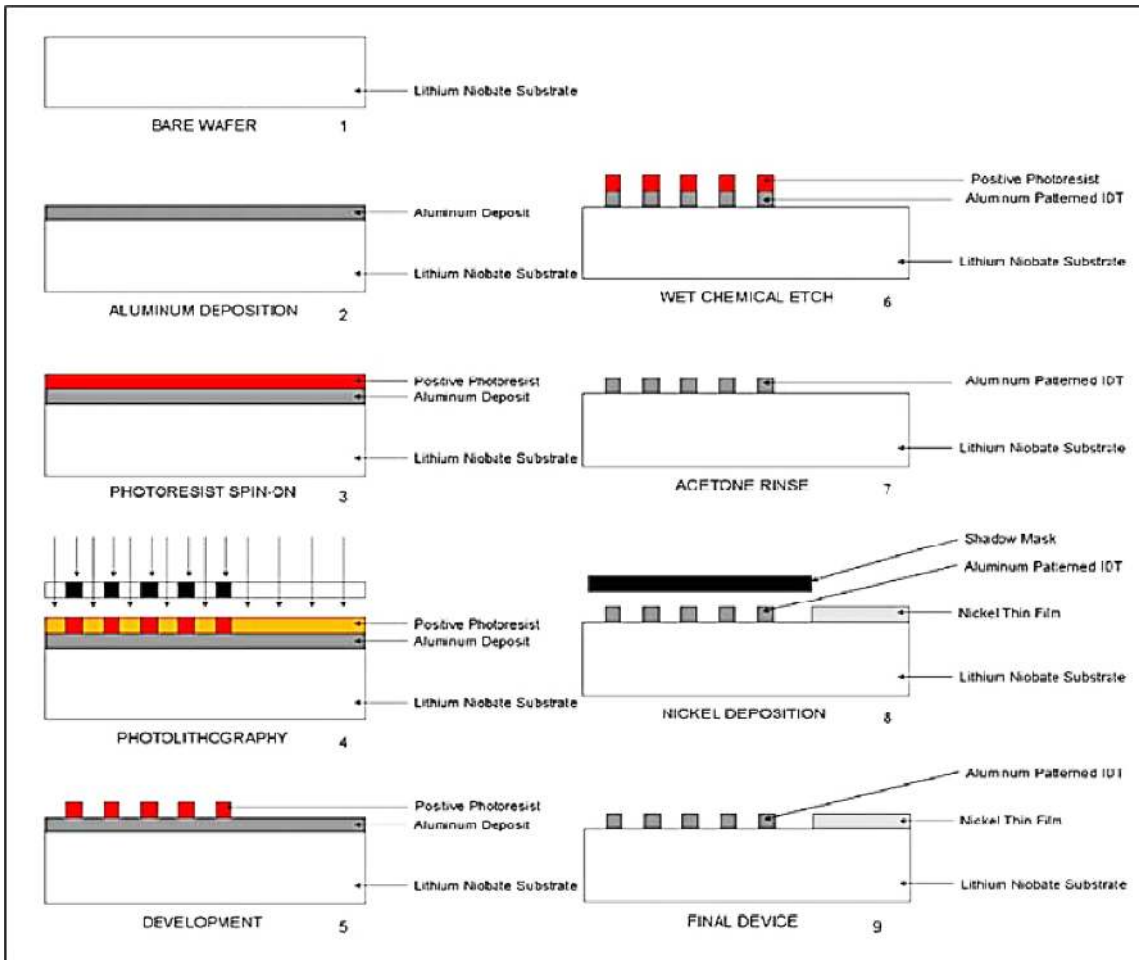

Fig. 16. (Color online) The fabrication process of thin film based SAW magnetic sensor (shown left half part only).

underneath. The exposed metal layer is removed by etching away the metal while the portion of metal under the photoresist material remains. The protective photoresist layer is then removed using acetone.

Step 5: Wafer cleansing

The wafer is cleaned again to remove the containments and prepare for the thin film deposition step.

Step 6: Thin film deposition

A shadow mask is used to cover the entire wafer except for the region where the thin film has to be deposited. The thin film of magnetostrictive material, e.g. Nickel (Ni), is then deposited in the desired portion using Evaporation/ Sputtering/ chemical vapor deposition (CVD) process.

4. Conclusion

This paper discussed the potential use of SAW magnetic sensors and highlighted the most common design methodologies as reported in the literature. It also explained the process steps for fabricating a typical SAW magnetic sensor. SAW devices have a simple design and can be transformed into magnetic sensors by slight alterations in their structure. It is possible to achieve magnetic sensing ability either by depositing a magnetostrictive thin film in a SAW delay line, integrating GMI elements with the SAW reflectors or by using magnetostrictive SAW IDT. All these measures are ways to manipulate SAW characteristics in the presence of a magnetic field, which is the sole measurement principle for measuring magnetic fields.

SAW magnetic sensors are gradually replacing conventional magnetic sensors for a wide range of applications due to modern fabrication technologies and methods that have resulted in higher sensitivity levels, simpler design and lower cost. Although SAW magnetic sensors have not yet been commercialized, they have proven their worth and the growing research interest in the domain indicates that they are foreseen as the next generation of magnetic sensors.

Acknowledgment

This research was supported by the National Nature Science Foundation of China under the NSFC Grant 51375118 and Shenzhen Government Funding JCYJ20140417172417097and JCYJ20160330161701343.

References

[1] M. J. Caruso, T. Bratland, C. H. Smith, and R. Schneider, Sensors-Peterborough **15**, 34 (1998).
[2] C. P. O. Treutler, Sens. Actuators A Phys. **91**, 2 (2001).
[3] Pavel Ripka, Journal of Physics **450**, 012001 (2013).
[4] J. Včelák, P. Ripka, and A. Zikmund, J. Supercond. Nov. Magn. **28**, 1077 (2015).
[5] T. Reininger, F. Welker, and M. Von Zeppelin, Sens. Actuators A Phys. **129**, 270 (2006).
[6] Z. Jia and R. D. K. Misra, Materials Technologies **26**, 191 (2011).
[7] G. Rivero, J. Spottorno, and M. Multigner, Magnetic Senors-Principles and Applications, Intech Open Access Publisher (2012).
[8] V. P. Bui, O. Chadebec, L. L. Rouve, and J. L. Coulomb, IEEE Trans. Magn. **44**, 1050 (2008).
[9] J. W. Wilson, G. Y. Tian, and S. Barrans, Sens. Actuators A Phys. **135**, 381 (2007).
[10] Lenz James and S. Edelstein, IEEE Sensors J. **6**, 631 (2006).
[11] P. Ripka, Sens. Actuators A Phys. **106**, 8 (2003).
[12] D. S. Benitez, Sung Quek, Patrick Gaydecki, and Vladimir Torres, IEEE Trans. Instrum. Meas. **57**, 2437 (2008).
[13] J. Clarke and A. I. Braginski, The SQUID Handbook, 391 (2004).
[14] Rhouni Amine, Gérard Sou, Paul Leroy, and Christophe Coillot, IEEE Sens. J. **13**, 159 (2013).
[15] Simpkins Alex and Emanuel Todorov, Proceedings of the 2010 American Control Conference, 1948 (2010).
[16] Bica Ioan, J. Ind. Eng. Chem. **17**, 83 (2011).
[17] Kubik Jan, Jan Vcelak and Pavel Ripka, Sens. Actuators A Phys. 129 (2006).
[18] Tondra Mark, J. M. Daughton, Dexin Wang, R. S. Beech, Anita Fink, and J. A. Taylor, J. Appl. Phys. **83**, 6688 (1998).
[19] Reig Candid, S. Cardoso, and Subhas Chandra Mukhopadhyay, Giant Magnetoresistance (GMR) Sensors. Springer Berlin Heidelberg (2013).
[20] Gad-el-Hak Mohamed, The MEMS Handbook, CRC Press (2001).
[21] D. Niarchos, Sens. Actuators A Phys. **109**, 166 (2003).
[22] Todaro Maria Teresa, Leonardo Sileo, and Massimo De Vittorio, Magnetic Senors-Principles and Applications Intech Open Access Publisher (2012).
[23] J. G. Rodriguez-Madrid, G. F. Iriarte, O. A. Williams, and F. Calle, Sens. Actuators A Phys. **189**, 364 (2013).
[24] A. Binder and R. Fachberger, IEEE Sens. J. **11**, 966 (2011).
[25] M. W. Gallagher and D. C. Malocha, IEEE Trans. Ultrason., Ferroelectrics and Frequency Control **60**, 596 (2013).
[26] Kalinin Victor, IEEE Int. Ultrason. Symp., 212 (2011).
[27] M. S. Nieuwenhuizen and A. J. Nederlof, Sens. Actuators B Chem. **2**, 97 (1990).
[28] A. Buvailo, Y. Xing, J. Hines, and E. Borguet, Sens. Actuators B Chem. **156**, 444 (2011).
[29] Transense Technologies plc: http://www.transense.co.uk/SAW/benefits-of-saw.html (2009).
[30] L. Reindl, G. Scholl, T. Ostertag, C. C. W. Ruppel, W. E. Bulst, and F. Seifert, IEEE Ultrason. Symp. Proc. **1**, 363 (1996).
[31] Pohl Alfred, IEEE Transactions on Ultrasonics, Ferroelectrics and Frequency Control **47**, 317 (2000).
[32] B. Q. Liu and C. R. Zhan, IEEE Symposium on Piezoelectricity, Acoustic Waves, and Device Applications (SPAWDA), 59 (2015).
[33] Lehtonen Saku, Optimization of reflector and transducer properties for surface acoustic wave devices on 128° $LiNbO_3$ Helsinki University of Technology (2004).
[34] J. Z. Song, P. Bai, Z. H. Hang, and Yun Lai, New Journal of Physics **16**, 033026 (2014).
[35] Morgan David, Surface acoustic wave filters: With applications to electronic communications and signal processing, Academic Press (2010).
[36] S. Gong, L. Shi, and G. Piazza, IEEE Microwave Symposium Digest (MTT), 1 (2012).
[37] G. Bu, D. Ciplys, M. Shur, L. J. Schowalter, S. Schujman, and R. Gaska, Appl. Phys. Letter. **84**, 4611 (2004).
[38] G. Bu, D. Ciplys, M. Shur, L. J. Schowalter, S. Schujman, and R. Gaska, IEEE Transactions on Ultrasonics, Ferroelectrics and Frequency Control **53**, 251 (2006).
[39] C. S. Lam, C. Y. J. Wang, and S. M. Wang, Proceedings of the Fourth International Symposium on Acoustic Wave Devices for Future Mobile Communication Systems, 3 (2010).
[40] Campbell Colin, Surface acoustic wave devices for mobile and wireless communications, Academic Press, (1998).
[41] R. C. Jaeger, Introduction to Microelectronic Fabrication, Prentice Hall (2002).
[42] S. Fujii, T. Odawara, H. Yamada, T. Omori, K. Hashimoto, H. Torii, H. Umezawa, and S. Shikata, IEEE Transactions on Ultrasonics, Ferroelectrics, and Frequency Control **60**, 986 (2013).
[43] C. Gruber, A. Binder, and M. Lenzhofer, Second International Summit, IoT 360° 2015, Revised selected papers II, Springer International Publishing, 373 (2016).
[44] A. G. Olabi and A. Grunwald, Mater. Des. **29**, 469 (2008).
[45] K. H. J. Buschow and F. R. Boer, Physics of Magnetism and Magnetic Materials, Kluwer Academic/Plenum Pub-

lishers (2003).
[46] J.B.Thoelke, Magnetization and magnetostriction in highly magnetostrictive materials. Ames Lab., IA, United States (1993).
[47] M. J. Dapino, Struct. Eng. Mech. J. **17**, 1 (2002).
[48] A. K. Ganguly, K. L. Davis, D. C. Webb, C. Vittoria, and D. W. Forester, Electronics Letters **11**, 610 (1975).
[49] V. Koeninger, Y. Matsumura, H. H. Uchida, and H. Uchida, J. Alloys Compd. **211**, 581 (1994).
[50] A. E. Clark, M. Wun-Fogle, J. B. Restorff, and T. A. Lograsso, Mater. Trans. **43**, 881 (2002).
[51] A. E. Clark, J. B. Restorff, M. Wun-Fogle, T. A. Lograsso, and D. L. Schlagel, IEEE Trans. Magn. **36**, 3238 (2000).
[52] E. M. Summers, T. A. Lograsso, J. D. Snodgrass, and J. C. Slaughter, Smart Structures and Materials, International Society for Optics and Photonics **5387**, 448 (2004).
[53] W. Li, P. Dhagat, and A. Jander, IEEE Trans. Magn. **48**, 4100 (2012).
[54] H. F. Tiersten and B. K. Sinha, J. Appl. Phys. **49**, 87 (1978)
[55] H. Zhou, A. K. Talbi, N. Tiercelin, and O. BouMatar, Appl. Phys. Lett. **104**, 114101 (2014).
[56] M. Elhosni, S. Petit-Watelot, M. Hehn, S. Hage-Ali, K. A. Aissa, D. Lacour, A. Talbi, and O. Elmazria, Procedia Engineering **120**, 870 (2015).
[57] N. Y. Kozlovski and D. C. Malocha, IEEE Int. Ultrason. Symp. 1541 (2009).
[58] L. Reindl, G. Scholl, T. Ostertag, C. C. W. Ruppel, W. E. Bulst, and F. Seifert, IEEE Ultrasonics Symposium, Proceedings **1**, 363 (1996).
[59] L. Xie, T. Wang, P. Wang, and Jianchun Xing, Journal of Sensors 2016 (2016).
[60] M. H. Phan and H. X. Peng, Progress in Materials Science **53**, 323 (2008).
[61] M. Hauser, L. Kraus, and P. Ripka, IEEE Instrum. Meas. Mag. **4**, 28 (2001).
[62] H. X. Peng, F. Qin, and M. H. Phan, Ferromagnetic Microwire Composites, Springer International Publishing (2016).
[63] B. Li, H. Rowais, and J. Kosel, Modeling and Measurement Methods for Acoustic Waves and for Acoustic Microdevices, Intech Open Access Publisher (2013).
[64] B. Li, N. P. M. Salem, I. Giouroudi, and J. Kosel, J. Appl. Phys. **111**, 07E514 (2012).
[65] H. Hauser, J. Steurer, J. Nicolics, and I. Giouroudi, Wireless Magnetic Field Sensor (2006).
[66] M. Kadota, S. Ito, Y. Ito, T. Hada, and K. Okaguchi, Japanese J. Appl. Phys. **50**, 07HD07 (2011).
[67] M. Kadota and Shigeo Ito, Jpn. J. Appl. Phys. **51**, 07GC21 (2012).
[68] M. L. Chin, Oregon State University University (2006). http://ir.library.oregonstate.edu/xmlui/handle/1957/2336